

# Supporting Information

## **Intermetallic PdCu<sub>3</sub> Supported on Nanodiamond-Graphene for Semi-hydrogenation of Phenylacetylene**

Xiaoran Niu,<sup>a,b</sup> Ao Wang,<sup>b</sup> Lei Tong,<sup>\*b</sup> Lei Wang,<sup>c</sup> Yuan Kong,<sup>\*b</sup> Chenliang Su<sup>a</sup> and Hai-Wei Liang<sup>\*b</sup>

<sup>1</sup> International Collaborative Laboratory of 2D Materials for Optoelectronic Science & Technology of Ministry of Education, Institute of Microscale Optoelectronics, Shenzhen University, Shenzhen 518060, China;

<sup>2</sup> Hefei National Research Center for Physical Sciences at the Microscale, Department of Chemistry, University of Science and Technology of China, Hefei, 230026, China.

<sup>3</sup> School of Chemistry and Chemical Engineering, Yangzhou University, Yangzhou, Jiangsu 225009, China.

E-mail: ltong17@mail.ustc.edu.cn (L. Tong); kongyuan@ustc.edu.cn; hwliang@ustc.edu.cn (H.-W. Liang).

## Experimental section

The TOF calculation methods were provided in supporting information.

$$TOF (h^{-1}) = \frac{\text{rate of product formation (styrene)}}{\text{mole of active site}} \quad (1)$$

The Pd loading is used as the number of active sites in the TOF calculation process.

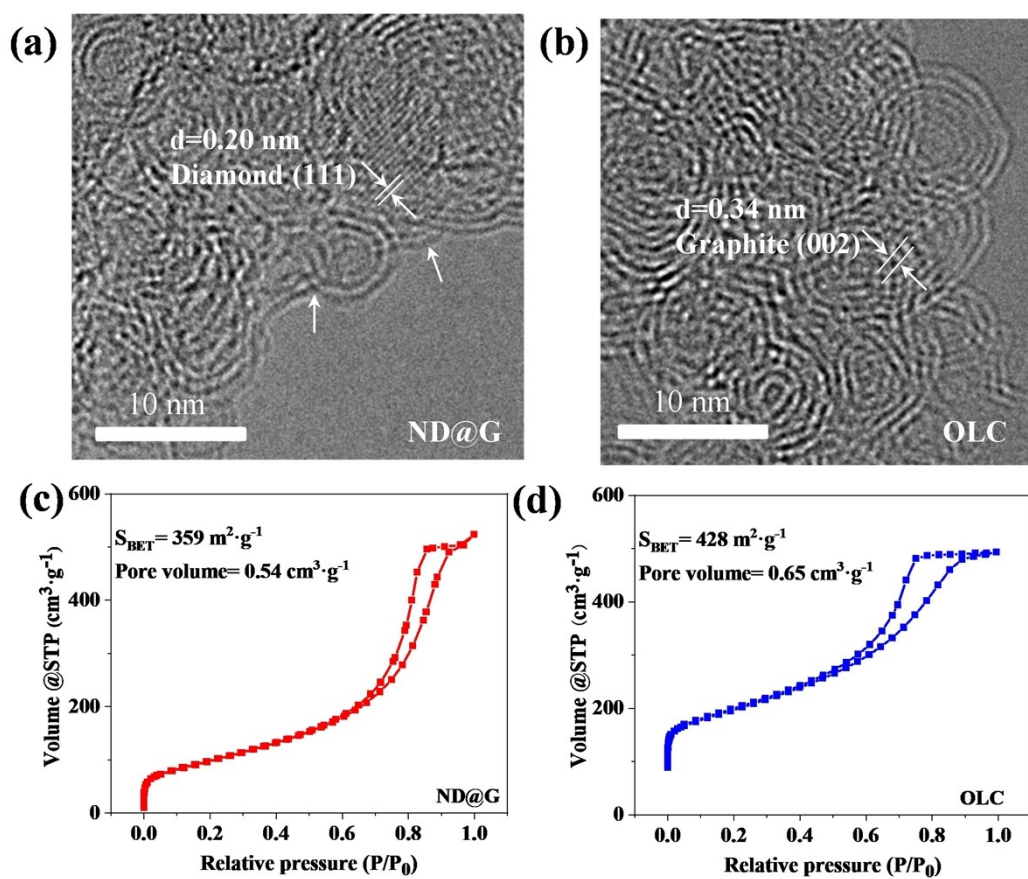


Figure S1. (a, b) HRTEM images of ND@G (a) and OLC (b). (c, d) Nitrogen adsorption-desorption isotherms of ND@G (c) and OLC (d).

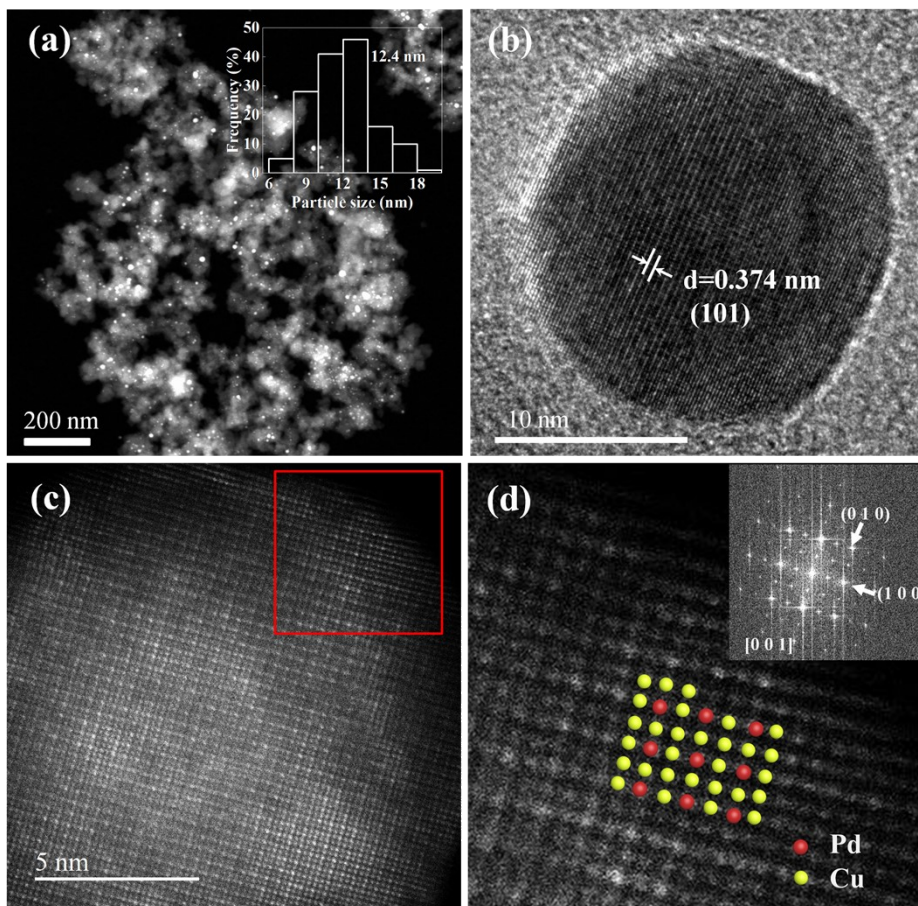


Figure S2. HADF-STEM (a,c,d) and HRTEM (b) images of PdCu<sub>3</sub>/ND@G; insets in a and d are the corresponding particle size distribution and the FFT pattern of PdCu<sub>3</sub>/OLC.

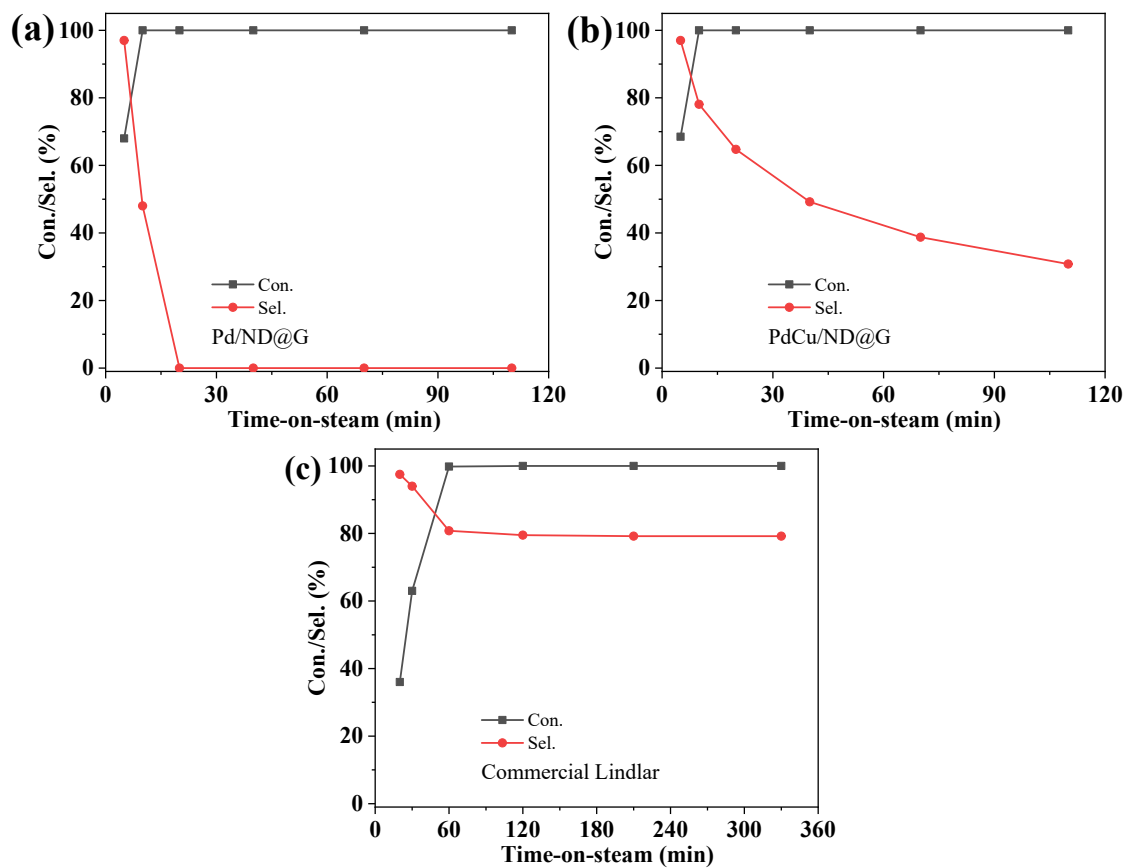


Figure S3. (a-c) Time-on-stream conversion and selectivity of phenylacetylene over Pd/ND@G (a), PdCu/ND@G (b), and commercial Lindlar catalysts (c).

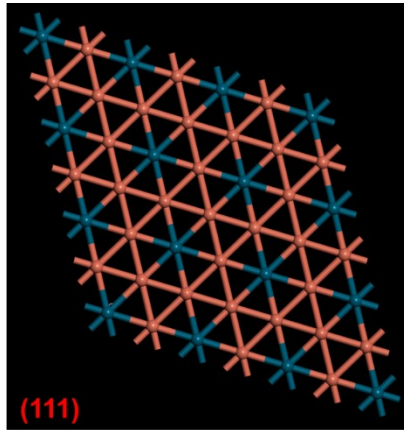


Figure S4. The (111) plane of intermetallic PdCu<sub>3</sub>

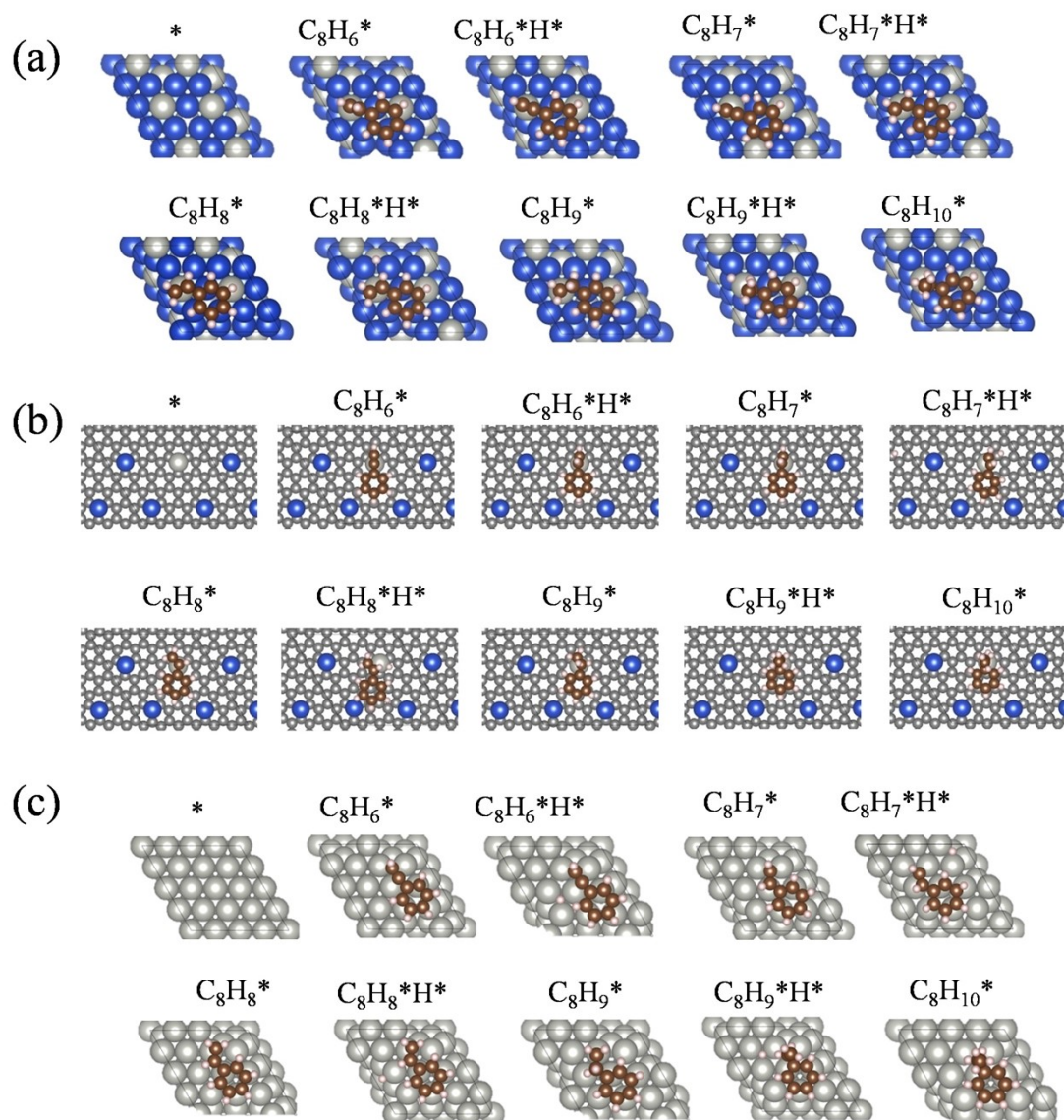


Figure S5. (a-c) Pictorial models for PdCu<sub>3</sub>/OLC (a), PdCu<sub>3</sub>/ND@G (b), and Pd (c), and their corresponding adsorption structure of C<sub>8</sub>H<sub>6</sub><sup>\*</sup>, C<sub>8</sub>H<sub>6</sub><sup>\*</sup>H<sup>\*</sup>, C<sub>8</sub>H<sub>7</sub><sup>\*</sup>, C<sub>8</sub>H<sub>7</sub><sup>\*</sup>H<sup>\*</sup>, C<sub>8</sub>H<sub>8</sub><sup>\*</sup>, C<sub>8</sub>H<sub>8</sub><sup>\*</sup>H<sup>\*</sup>, C<sub>8</sub>H<sub>9</sub><sup>\*</sup>, C<sub>8</sub>H<sub>9</sub><sup>\*</sup>H<sup>\*</sup>, and C<sub>8</sub>H<sub>10</sub><sup>\*</sup>.

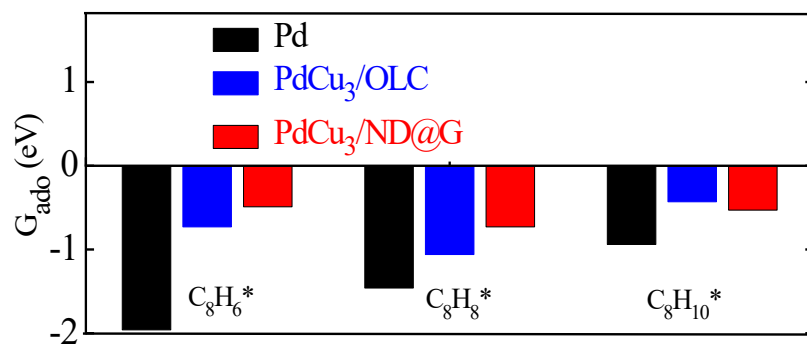


Figure S6. the adsorption energetics of C<sub>8</sub>H<sub>6</sub>\* , C<sub>8</sub>H<sub>8</sub>\* , and C<sub>8</sub>H<sub>10</sub>\* on Pd, PdCu<sub>3</sub>/OLC, and PdCu<sub>3</sub>/ND@G.



Table S1. The change in Gibbs free energy for each elementary reaction.

$\Delta G$	Pd	PdCu <sub>3</sub> /OLC	PdCu <sub>3</sub> /ND@G
$\Delta G_1$	1.96	0.73	0.49
$\Delta G_2$	0.28	0.15	0.55
$\Delta G_3$	0.41	0.87	1.19
$\Delta G_4$	0.46	0.04	0.31
$\Delta G_5$	0.19	1.11	1.37
$\Delta G_{6a}$	0.41	0.19	0.49
$\Delta G_{6b}$	1.46	1.06	0.73
$\Delta G_7$	0.27	0.01	0.3
$\Delta G_8$	1.16	1.16	1.76
$\Delta G_9$	1.42	1.63	2.67
$\Delta G_{10}$	0.94	0.43	0.53